



A physical reconstruction of solar magnetic field since 1700

J. Jiang^{1*} and D. Schmitt²

¹*Key Laboratory of Solar Activity, National Astronomical Observatories, Chinese Academy of Sciences, Beijing 100012, China*

²*Max-Planck-Institut für Sonnensystemforschung, 37191 Katlenburg-Lindau, Germany*

Abstract. We use the observed Royal Greenwich Observatory photoheliographic results to obtain the statistical properties of sunspot group emergence. These include correlations between the sunspot numbers and sunspot group latitudes, longitudes, areas and tilt angles. The semi-synthetic records of emerging sunspot groups were taken as input for a surface flux transport model to reconstruct the evolution of the large-scale solar magnetic field and the open heliospheric flux from the year 1700 onward. The reconstruction results for the total surface flux, the polar field, and the heliospheric open flux agree well with the available observational or empirically derived data and reconstructions. We confirm a significant positive correlation between the polar field during activity minimum periods and the strength of the subsequent sunspot cycle, which has implications for flux transport dynamo models for the solar cycle.

Keywords : Sun: evolution – Sun: activity

1. Introduction

The knowledge of the solar magnetic field during past centuries is of great interest not only for solar physicists as it provides a better understanding of the Sun itself, but also for geophysicists and climatologists because of the influences which the Sun has on our planet. The longest direct solar activity index is the relative sunspot number, which starts from 1700 for the Wolf sunspot number R_Z and from 1610 for the group

*email: jiejiang@nao.cas.cn

sunspot number R_G . Hence we use a physical model with the input of R_G or R_Z to reconstruct the solar magnetic field since 1700.

Solar surface flux transport model (SFTM) was initiated in the 1960s (Babcock 1961; Leighton 1964). Being refined during the past 40 yrs, the model well simulates the evolution of the magnetic field over the solar surface (Wang, Nash & Sheeley 1989; Mackay, Priest & Lockwood 2002; Schüssler & Baumann 2006; Schrijver & Liu 2008). It describes the passive transport of the radial component of the magnetic field, B , under the effect of differential rotation, Ω , meridional flow, v , and turbulent surface diffusivity, η_H . A possible slow decay due to the fact that diffusion occurs in three dimensions is introduced by a radial diffusion coefficient η_r (for details, see Cameron et al. 2010; Jiang et al. 2010).

The source term of the magnetic flux in the governing equation of the surface flux transport model describes the emergence of bipolar magnetic regions as a function of latitude λ , longitude ϕ and time t . To derive this term for simulations, we have to know the area, location and tilt angle of each sunspot group. Hence we need to construct the synthetic datasets of sunspot group emergence using sunspot number. In the following, we mainly use the R_G data.

2. Characteristics of sunspot group emergence and reconstruction of the butterfly diagram

In this section we discuss the empirical relationships between the cycle strength S_n derived from R_G and the latitudes, longitudes and areas of sunspot groups as recorded in the Royal Greenwich Observatory (RGO) dataset from 1874 to 1976 and tilt angles of sunspot groups as recorded in Mount Wilson and Kodaikanal observatories from 1913 to 1986. For the details to get the correlations see Jiang et al. (2011a).

The cycle strength S_n is defined as the maximum of the 12 month running mean of R_G . The relation between the cycle averaged latitudes λ_n and S_n obeys $\lambda_n = 12.2 + 0.022S_n$. We break the time between adjacent minima into 30 equal phases. At the i th phase bin, the dependence of the mean latitude of emergence for different cycles n is $\lambda_n^i = (26.4 - 34.2(i/30) + 16.1(i/30)^2)(\lambda_n / < \lambda >_{12-20})$ for $0 \leq i \leq 30$ and where $< \lambda >_{12-20} = 14.6^\circ$ is the average latitude of sunspot emergence over all the cycles. We consider the standard deviation, σ_n^i , of the latitudinal distribution during phase i of cycle n being proportional to the width of the latitude distribution, which may be expressed as $\sigma_n^i = (0.14 + 1.05(i/30) - 0.78(i/30)^2)\lambda_n^i$.

The emergence longitudes of sunspot groups is known to be not entirely random. By comparing a proxy for the equatorial dipole moment for the random and the observed models for the longitude distribution of sunspot emergence, we confirmed the existence of active longitudes. This means that we should include the non-randomness

of longitude distribution in the reconstruction since the open flux of the Sun during activity maxima is dominated by the equatorial low order multipoles.

Concerning the area distribution, the number density function of sunspot group areas is approximately a power law below $300 \mu\text{Hem}$ with a turnover to an almost log-normal distribution above. There is a large range (from 60 to $300 \mu\text{Hem}$) where both functional forms are good approximations to the data and the number density function is cycle independent, which means the distribution of emerging flux is similar in all cycles. The cycle phase dependence of area distribution can be fitted by the second degree polynomial $A_i = 115 + 396(i/30) - 426(i/30)^2$.

The tilt angles of sunspot groups from Mount Wilson Observatory and from Kodaikanal observations, show that the average tilt angle is negatively correlated with the strength of the cycle (Dasi-Espuig et al. 2010). We take the dependence of the tilt angle on latitude as a square root profile $\alpha_n = T_n \sqrt{|\lambda|}$ where α_n is the average tilt angle and T_n is the constant of proportionality for cycle n . The linear fit between S_n and T_n is $T_n = 1.73 - 0.0035S_n$.

We have used R_G to determine strength of each cycle and have found correlations which allow us to construct synthetic latitudes, longitudes, areas and tilt angles for each spot group. We here determine how many sunspot groups should appear each month to make the semi-synthetic record have similar statistics as the RGO dataset. For the period covered by the RGO records, the monthly number should be approximately the same as the number of groups in the RGO dataset, N_{SG} . We have found that $N_{SG} = R_G/2.1$ matches the data well. We use this fit to reconstruct the number of sunspot groups appearing each month from 1700 onwards.

3. Solar surface flux transport model and extrapolation

The three parameters, differential rotation, meridional flow and surface diffusivity in the governing equation of the SFTM follow the profiles given in Cameron et al. (2010). We also use the same methods to treat the initial field distribution and the source magnetic flux of each sunspot group.

Due to different observers and different calibrations, sunspot number datasets are less reliable before 1849 (Vaquero 2007), which affect our reconstructed magnetic field. If $\eta_r = 0$, the polar field generated by the evolution of flux emergence reaches a nearly steady balance under the effect of surface diffusion and poleward meridional flow (decay time about 4000 yrs). Thus an overestimated or an underestimated polar field persists through the whole simulations. Hence we introduce a weak radial diffusivity $\eta_r = 25 \text{ km}^2\text{s}^{-1}$ (decay time about 20 yrs) to diminish the effect caused by a possible uncorrect sunspot number in one cycle on its subsequent cycles.

The SFTM describes the evolution of the magnetic field on the Sun's surface. To

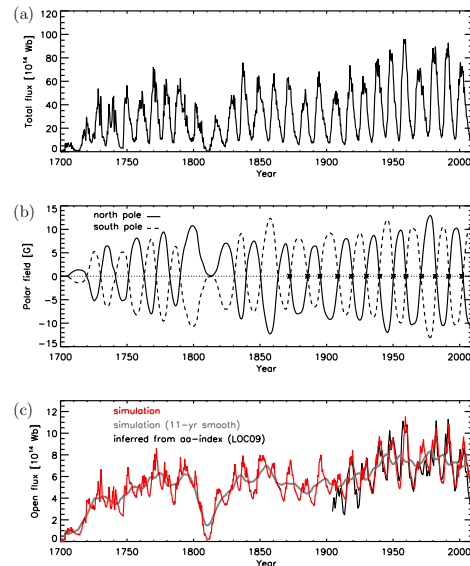


Figure 1. Results with R_G during 1700–2010. The first 20 years are affected by the arbitrary initial magnetic field. (a). Total flux. (b). Polar field. Solid and dashed curves are for the northern and southern hemisphere, respectively. (c). Open flux. The Red curve shows the simulated result. The grey curve is a 11-yr running average. The black curve is inferred from the geomagnetic indices with kinematic correction (LOC09).

obtain the heliospheric open flux we have to extrapolate the surface field outward. What we use is the current sheet source surface (CSSS) extrapolation (Zhao & Hoeksema 1995a,b).

4. Time evolution of the reconstructed field since 1700

Figure 1 shows the reconstructed solar magnetic field based on R_G , including total flux (a), polar field (b) and open flux (c). The polar field displays regular reversals, except during the Dalton minimum, when a reversal appears to fail. The flux transported to the poles during the weak cycle 5 just cancels the strong polar field generated by the strong and long cycle 4. The grey curves in Panels (c) of Fig. 1 are the 11-yr running average of the open flux. The long-term trend is compared with other independent reconstructions in Fig. 2.

Figure 2 shows the comparison of our 11-yr running average of the reconstructed open flux since 1700 (Red: R_G ; Blue: R_Z) with other methods, which are based on the geomagnetic indices by Lockwood et al. (2009, LOC09) and Svalgaard & Cliver (2010, SC10), on the cosmogenic radionuclide data by McCracken (2007, McC07)

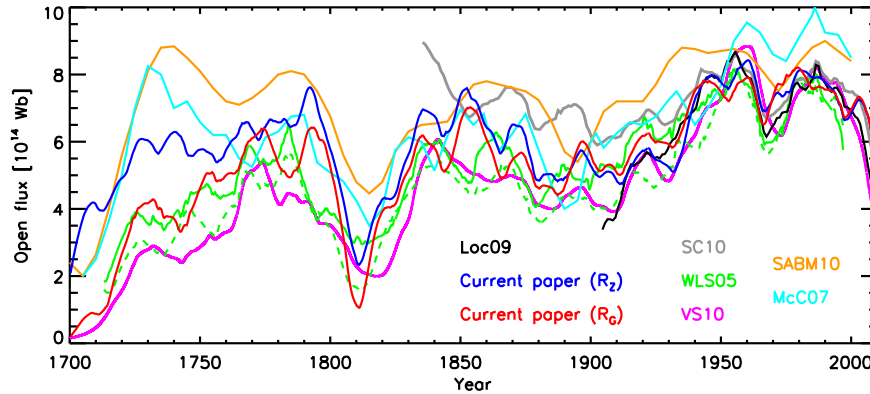


Figure 2. Comparison of our reconstructed open flux (Red: R_G ; Blue: R_Z) with other reconstructions since 1700. Loc09: Lockwood et al. (2009); WLS05: Wang et al. (2005); solid and dashed green are their models S1 and S2, respectively. SC10: Svalgaard & Cliver (2010). A factor 0.4 is used to convert their result. VS10: Vieira & Solanki (2010). SABM10: Steinhilber et al. (2010), their PCA composite. McC07: McCracken (2007).

and Steinhilber et al. (2010, SABM10) and on the sunspot number data by Vieira & Solanki (2010, VS10) and Wang et al. (2005, WLS05). Our constructed open flux corresponds to the radial component of the magnetic field near the earth. Since the values given in SC10 are the heliospheric magnetic field amplitude, a factor 0.4 is used to convert it to the radial component and then to get the open flux. Our reconstructed values are among the different results.

By analyzing the correlations between sunspot numbers and the reconstructed solar magnetic field, we get the results that the total flux is roughly proportional to the sunspot number. The polar fields show both correlations with the strength of the same cycle and of the next cycle. According to the numerical experiment during the reliable time period of sunspot number data (1874 onwards), the correlation between the polar field and the next cycle would be stronger than the case without the radial diffusivity. The open flux at the solar maximum is proportional to the sunspot number and the correlation becomes weaker during the minimum. For the details see Jiang et al. (2011b).

5. Conclusion

We provide a physical reconstruction of the large-scale solar magnetic field and the open heliospheric flux since 1700 with a surface flux transport model with sources based on sunspot number data and on the statistical properties of the sunspot groups in the RGO photoheliographic results. The model has been validated through compar-

ison with reconstructions based on the actual sunspot group records and with directly measured or observationally inferred quantities.

The reconstructions considerably extend the basis for correlations studies, such as the relation between the polar field amplitude during activity minima and the strengths of the preceding and subsequent cycles, with implications for dynamo models.

Acknowledge

JJ thanks the organizers of the first Asia-Pacific Solar Physics Meeting. The National Basic Research Program of China through grants 10703007, 10733020 and the Young Researcher Grant of National Astronomical Observatories, Chinese Academy of Sciences are acknowledged for the partial funding of JJ's research.

References

- Babcock H. W., 1961, *ApJ*, 133, 572
Cameron R. H., Jiang J., Schmitt D., Schüssler M., 2010, *ApJ*, 719, 264
Dasi-Espuig M., Solanki S. K., Krivova N. A., Cameron R., Peñuela T., 2010, *A&A*, 518, A7
Jiang J., Cameron R. H., Schmitt D., Schüssler M., 2010, *ApJ*, 709, 301
Jiang J., Cameron R. H., Schmitt D., Schüssler M., 2011a, *A&A*, 528, A82
Jiang J., Cameron R. H., Schmitt D., Schüssler M., 2011b, *A&A*, 528, A83
Leighton R. B., 1964, *ApJ*, 140, 1547
Lockwood M., Owens M., Rouillard A. P., 2009, *JGRA*, 114, 11104
Mackay D. H., Priest E. R., Lockwood M., 2002, *Solar Phys.*, 209, 287
McCracken K. G., 2007, *JGRA*, 112, 9106
Schüssler M., Baumann I., 2006, *A&A*, 459, 945
Schrijver C. J., Liu Y., 2008, *Solar Phys.*, 252, 19
Steinhilber F., Abreu J. A., Beer J., McCracken K. G., 2010, *JGRA*, 115, 1104
Svalgaard L., Cliver E. W., 2010, *JGRA*, 115, 9111
Vaquero J. M., 2007, *AdSpR*, 40, 929
Vieira L. E. A., Solanki S. K., 2010, *A&A*, 509, A100
Wang Y.-M., Nash A. G., Sheeley N. R., Jr., 1989, *ApJ*, 347, 529
Wang Y.-M., Lean J. L., Sheeley N. R., Jr., 2005, *ApJ*, 625, 522
Zhao X., Hoeksema J. T., 1995a, *AdSpR*, 16, 181
Zhao X., Hoeksema J. T., 1995b, *JGR*, 100, 19